SCIENTIFIC REPORTS

SUBJECT AREAS:
APPLIED PHYSICS
MODELLING AND THEORY
STATISTICAL PHYSICS, THERMODYNAMICS AND NONLINEAR DYNAMICS
INFORMATION THEORY AND COMPUTATION

Detection of hidden structures for arbitrary scales in complex physical systems

P. Ronhovde[1], S. Chakrabarty[1], D. Hu[1], M. Sahu[1], K. K. Sahu[2], K. F. Kelton[1], N. A. Mauro[1] & Z. Nussinov[1,3]

[1]Department of Physics, Washington University in St. Louis, Campus Box 1105, 1 Brookings Drive, St. Louis, MO 63130, USA, [2]Metal Physics and Technology, ETH, 8093 Zurich, Switzerland, [3]Kavli Institute for Theoretical Physics, Santa Barbara, CA 93106, USA.

Received
23 November 2011

Accepted
29 February 2012

Published
29 March 2012

Correspondence and requests for materials should be addressed to Z.N. (zohar@wuphys.wustl.edu)

Recent decades have experienced the discovery of numerous complex materials. At the root of the complexity underlying many of these materials lies a large number of contending atomic- and largerscale configurations. In order to obtain a more detailed understanding of such systems, we need tools that enable the detection of pertinent structures on all spatial and temporal scales. Towards this end, we suggest a new method that applies to both static and dynamic systems which invokes ideas from network analysis and information theory. Our approach efficiently identifies basic unit cells, topological defects, and candidate natural structures. The method is particularly useful where a clear definition of order is lacking, and the identified features may constitute a natural point of departure for further analysis.

Currently, no universal tools exist for examining complex physical systems in a general and systematic way that fleshes out their pertinent features, from the smallest fundamental unit to the largest scale encompassing the entire system. The challenge posed by these complex materials is acute and stands in stark contrast to simple ordered systems. In crystals, atomic unit cells replicate to span the entire system. Historically, the regular shapes of some large-scale single crystals were suggested to reflect the existence of an underlying repetitive atomic scale unit cell structure long before modern microscopy and the advent of scattering and tunneling techniques. This simplicity enables an understanding of many solids in great detail; but in complex systems, rich new structures may appear on additional intermediate scales.

Currently, some of the oldest and most heavily investigated complex materials are glasses. Recent challenges include the high temperature cuprate and pnictide superconductors, heavy fermion compounds, and many other compounds including the manganites, the vanadates, and the ruthenates. These systems exhibit a wide array of behavior including superconductivity and metal to insulator transitions, rich magnetic characteristic and incommensurate orders, colossal magneto-resistance, orbital orders, and novel transport properties.

A wealth of experimental and numerical data has accumulated on such systems. The discovery of the salient features in such complex materials and more generally of complex large scale physical systems across all spatial resolutions may afford clues to develop a more accurate understanding of these systems. In disparate arenas, guesswork is often invoked as to which features of the systems are important enough to form the foundation for a detailed analysis. With ever-increasing experimental and computational data, such challenges will only sharpen in the coming years. There is a need for methods that may pinpoint central features on all scales, and this work suggests a path towards the solution of this problem in complex amorphous materials. A companion work[1] provides many details that are not provided in this brief summary. An explanation of our core ideas require a few concepts from the physics of glasses and network analysis.

Results

We illustrate our approach by reviewing a central problem—the detection of natural scales and structures in glasses. Such complex systems are not easy to analyze with conventional theoretical tools[2]. In a gas, all interactions between the basic constituents are weak, so the system is easy to understand and analyze. At the other extreme, the interactions in regular periodic solids are generally strong, and such solids may be characterized by their unit cells and related broken symmetries.

The situation is radically different for liquids and glasses. Liquids that are rapidly cooled ("supercooled") below their melting temperature cannot crystallize and instead, at sufficiently low temperatures, become "frozen" in an

amorphous state (a "glass") on experimental times scales. On supercooling, liquids may veer towards local low energy structures[3,4], such as icosahedral structures observed in metallic glasses[5,6], before being quenched into the amorphous state. Lacking a simple crystalline reference, the general structure of glasses (especially prevalent multi-component glasses) is notoriously difficult to quantify in a meaningful way beyond the smallest local scales. As such, it remains a paradigm for analyzing structure in complex materials.

The most familiar and oldest technological glasses are the common silicate glasses. More modern glasses include phosphate (biomedical applications), semiconductor chalcogenide (optical recording media), and metallic glasses. Glass formers display several key features[7]. One prominent aspect is that the viscosity and relaxation times increase by many orders of magnitude over a narrow temperature range. This dynamic sluggishness is not accompanied by normal thermodynamic signatures of conventional phase transitions nor a pronounced change of spatial structure. The high number of metastable energy states in these systems[8,9] leads to rich energy landscapes[8–12]. A notable facet of the glass transition in the space-time domain is that the dynamics of supercooled liquids are not spatially uniform ("dynamical heterogeneities")[13].

Many theories of glasses, e.g.,[7,14–21] have been advanced over the years. The theory of Random First Order Transitions (RFOT) investigates mosaics of local configurations[7,14]. As shown in[19], RFOT is related to theories of "locally preferred structures"[20,22–24]—which also rely on the understanding of natural structures in glasses. Other (inter-related) theories seek a similar quantification of structure. Investigations include spin glass approaches[15] topological defects and kinetic constraints[19,20,25–27], network topology[28], and numerous approaches summarized in excellent reviews, e.g.,[11,29,30].

There is a proof that a growing static length scale must accompany the diverging relaxation times of glass[31]. Some evidence has been found supporting the existence of growing correlation lengths (associated with both static correlations as well as those describing dynamic inhomogeneities)[32,33]. More recent discussions include divergent shear penetration depths[1]. Correlation lengths were studied via "point-to-set" correlations[34] and pattern repetition size[35]. Common methods of characterizing structures center on an atom or a given link: (a) Voronoi polyhedra,[27,36]. (b) Honeycutt-Andersen indices[37], and (c) bond orientation[38]. A long-standing challenge addressed in this work is the direct detection of structures *of general character and scale* in amorphous physical systems. Towards this end, we briefly introduce several concepts from network analysis.

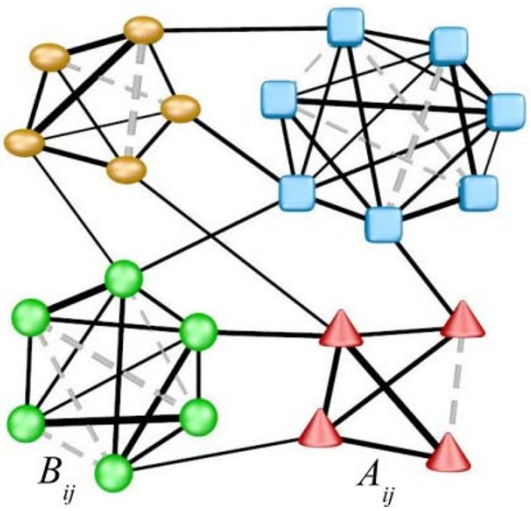

Figure 1 | A weighted network with 4 natural (strongly connected) communities. The goal in community detection is to identify such strongly related clusters of nodes. Solid lines depict weighted links corresponding to complimentary or attractive relationships between nodes i and j (denoted by A_{ij}) $[(V_{ij}-\upsilon)<0$ in Eq. (1)]. Gray dashed lines depict missing or repulsive edges (denoted by B_{ij}) $[(V_{ij}-\upsilon)>0]$. In both cases, the relative link weight is indicated by the respective line thicknesses.

Network analysis. Network analysis has been transformative in generating keen new insights in numerous areas such as sociology, homeland security, biology, and many other problems. Complex physical problems have not yet been examined before through this prism in this detail. We specifically introduce methods from the growing discipline of "community detection"[39]. The key idea is that any complex physical system may be expressed as a network of nodes (e.g., atoms, electrons, etc.) and connecting links that quantify the relations (interactions/correlations) between the nodes. With this representation, we then apply *multiresolution* methods[40] from network theory to analyze the systems.

Partitions of large systems into weakly coupled elements. As depicted in Fig. 1, community detection describes the problem of finding clusters ("communities") of nodes with strong internal connections and weak connections between different clusters. The definitions of nodes and edges depend on the system being modeled. For the present system, between each pair of nodes i and j we have an edge weight V_{ij} which may emulate an interaction energy or measured correlation between sites i and j. The nodes may belong to any of q communities, $\{C_a\}_{a=1}^{q}$. In our particular realization, the nodes represent particles and edges model the pair-wise potential energy interactions.

An ideal decomposition of a large graph is into completely disjoint communities (groups of particles) where there are no interactions between different communities. The system is effectively an "ideal gas" of the decoupled clusters. In practice, the task is to find a partition into communities which are maximally decoupled. Such a separation may afford insight into large physical systems. Many approaches to community detection exist[47].

Community detection method. We generalize our earlier works by adding a background ν and allowing for continuous weights V_{ij}. Our (Potts type) Hamiltonian reads

$$H=\frac{1}{2}\sum_{a=1}^{q}\sum_{i,j\in C_a}\left(V_{ij}-\nu\right)\left[\theta\left(\nu-V_{ij}\right)+\gamma\theta\left(V_{ij}-\nu\right)\right]. \qquad (1)$$

In Eq. (1), the inner sum is over nodes i and j in the same community C_a, and the outer sum is performed over the q different communities. The number of communities q may be specified from the outset or left arbitrary (the usual case) allowing the algorithm to determine q based on the lowest energy solution(s)[40,42].

Minimizing this Hamiltonian corresponds to identifying strongly connected clusters of nodes. The parameter $\gamma>0$ tunes the relative weights of the connected and unconnected edges and allows us to vary the targeted scale of the community division (the "resolution"). The model for the current application could be further generalized by incorporating n-body interactions or correlation functions (such as three or four point correlation functions). Details concerning a greedy minimization of Eq. (1) appear in[40,42]. Somewhat better optimization could be obtained with a heat bath algorithm[43] at a cost of substantially increased computational effort, but the greedy algorithm has shown itself to be robust.

Multiresolution network analysis. We address multi-scale partitioning[40] by employing information-theory measures[44,45] to examine contending partitions for each system scale. While decreasing γ, we minimize Eq. (1) resulting in partitions with progressively lower intra-community edge densities, effectively "zooming out" toward larger structures. A key construct in our approach is the application of *replicas*—independent solutions of the same problem. The

number of replicas p may be set by the user where higher value of p leads to more accurate analysis.

In earlier work[40], we dealt with a static network where replicas were formed by permuting the order of nodes for the same network definition. Here, we take advantage of the dynamic system to implement a further generalization where replicas are defined at different times. We automatically determine the natural scales of a system by identifying the values of γ for which these replicas agree most strongly via information theory measures such as normalized mutual information NMI and variation of information VI.

The central result in[40] was that *extrema* (including plateaux) of information theory overlaps (when averaged over all replica pairs) indicate the *"natural" network scales*[40]. That is, we find the values γ^* for which the average Q of information overlaps (over all replica pairs) is extremal, $(dQ/d\gamma)\big|_{\gamma=\gamma^*}=0$. We then identify the partitions that correspond to these γ^* (s).

This approach is fast[40,42] and has an accuracy that surpasses most methods, such as SA applied to other disparate cost functions[40,42]. More notably, to our knowledge, this approach is the only one that quantitatively evaluates the natural partitions for all scales. A detailed analysis[41] compared the accuracy of several algorithms for non multi-scale community detection. Multiresolution approaches[40,46,47] are much more recent. In the current analysis, we further apply a relatively trivial extension[1] that allows "overlapping" communities (nodes have more than one membership) to better model the physical clusters.

Detection of multi-scale structures in complex systems. We ascertain general hidden structure in complex systems with *no prior assumptions* regarding what the important properties may be. To achieve this, we set the graph edge weights for use Eq. (1) to be either (*i*) pair interaction energies or (*ii*) inter-node (inter-atomic) correlations[1] (see SI).

Our approach to multi-scale community detection[40] is conceptually simple: copies of the community detection problem are given to different "solvers" (or "replicas"). If the starting solution trajectories of the distinct replicas in the complex energy landscape are different, then they will generally arrive at different solutions (different community groupings). If many of the solvers strongly agree about certain features, then these aspects are more likely to be correct, and the level of agreement is measured by information theory correlations.

When applying this to a physical system, the replicas can be chosen to be copies of the system all at the same time. This setup will detect natural *static* scales and structures. Alternatively, the replicas may be copies of the system at different times, as depicted in Fig. 2, enabling the detection of general spatio-temporal correlations. In either case, we find the extrema of the information theory correlations as a function of γ the "resolution" parameter in our Hamiltonian Eq. (1). Once these extremal values are found, the ground states of Eq. (1) determine the pertinent structures. Multiple extrema in the information theory correlations suggest *multiple relevant length/time scales*. In this way, our analysis is not limited to the assumption of one or two specific correlation lengths relative to which scaling type analysis may be performed or what correlation function should be constructed. Rather, viable natural scales of the system appear as extrema in the calculation of the direct information theory overlaps.

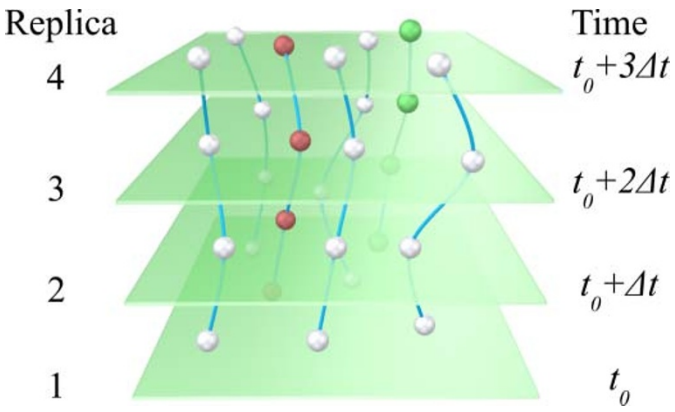

Figure 2 | A set of replicas separated by a time Δt between successive replicas. We generate a model network for each replica using the potential energy between the atoms as the respective edge weights and then solve each replica independently by minimizing Eq. (1) over a range of γ values. We then use information measures[40] to evaluate how strongly pairs of replicas agree on the ground states of Eq. (1).

Applications to complex amorphous systems. We used interaction energies to investigate a ternary metallic glass model $Al_{88}Y_7Fe_5$. At low temperatures, we found larger and more pronounced compact structures than those at higher temperature. Static and dynamic structures in the KA LJ glass are illustrated in the SI. *Large* atomic structures of $Zr_{80}Pt_{20}$ (based on RMC directly applied to experimental measurements) are shown in[1].

In Figs. 3 and 4, we provide the multiresolution plots at low and high temperatures, respectively. A sample of the corresponding structures of $Al_{88}Y_7Fe_5$ for the T = 300 K system are depicted in Fig. 5. These clusters are selected at the peak NMI at γ = 0.001. The identified structures are not unique reflecting a high configurational entropy. That is, different partitions may be found for a given value of the resolution parameter γ that are similar in their overall scale but different in precise detail and identities of the nodes. These results may flesh out a facet of the glass transition. As the system is

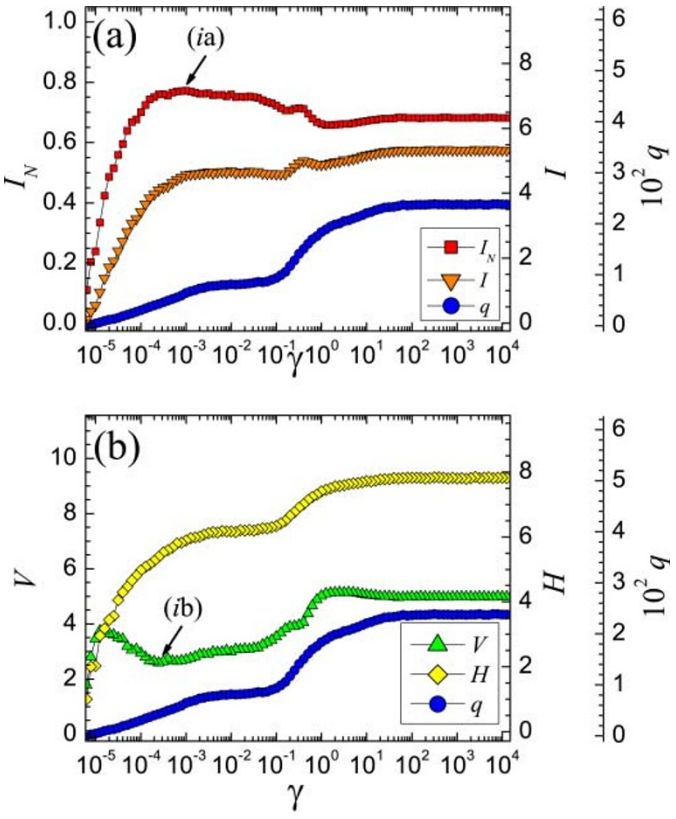

Figure 3 | The result of our community detection analysis applied to $Al_{88}Y_7Fe_5$ at a temperature of T = 300 K. The panels at left (a, b) show the information theoretic overlaps between the different replicas when averaged over all replica pairs (see text). In Fig. 5, we highlight the spatial structures corresponding to the NMI maximum/VI minimum.

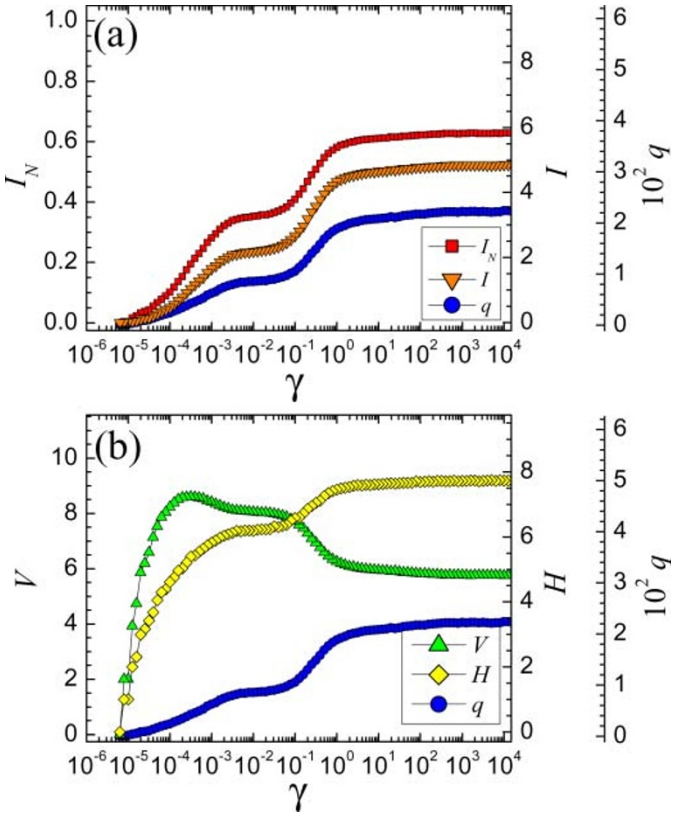

Figure 4 | The result of our community detection analysis as applied to $Al_{88}Y_7Fe_5$ at a temperature T = 1500 K. When comparing the information theory replica overlaps and structure with Fig. 3, it is evident that at higher temperatures, the system is more random.

supercooled, the effective couplings become quenched. Detecting the optimally decoupled structures, such as those that may describe the deeply supercooled liquid, constitutes a spin-glass problem[43].

Temperature dependence. We connect the network system to a large heat reservoir at a constant temperature T_{CD} and solve the community detection problem using a stochastic heat bath algorithm[43,48]. With this setup, any determined communities must have an interaction energy that is stable with respect to thermal fluctuations. Since the above results are at $T_{CD} = 0$ via a greedy solver, this effect was omitted above.

Since we base the edge weights on the interaction potentials, and the ϕ_0 shifts are relatively small here, we assign $T_{CD} \simeq T$ so that the community detection temperature is approximately equal to the simulation temperature. The caveat is that the "repulsive" energies in terms of Eq. (1) are scaled by the model weight γ, so the correspondence is best near $\gamma = 1$.

In Fig. 6, we plot the NMI (I_N) and the number communities q as a function of the heat bath temperature T_{CD} and Potts model

Figure 5 | A set of sample clusters found in a three dimensional AlYFe model system (see text). Here we allow for overlapping nodes. The information overlaps at left show a maximum NMI (I_N) and plateau for other information theory measures at (i) in Fig. 3.

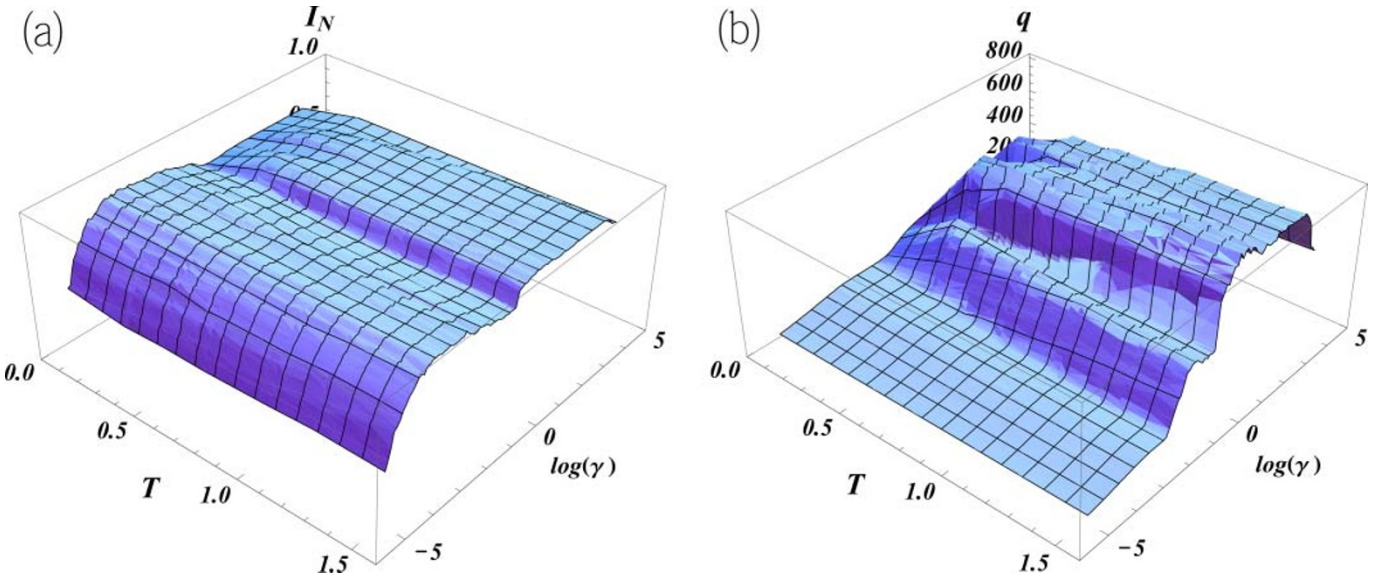

Figure 6 | Our community detection analysis is applied to the $Al_{88}Y_7Fe_5$ system at T = 300 K in panels (a) and (b) for a range of heat bath temperatures T_{CD} (temperature used for the community detection solver). Both panels here represent a single instant in time as opposed to the time varied replicas used in Figs. 3 and 4. Panel (a) plots NMI I_N, and panel (b) plots the corresponding number of clusters q. The sample clusters in Fig. 5 are found at the left edge of panel (a).

parameter γ[43,48]. In panels (a) and (b), we observe different phases with distinct transitions for $T_{CD} = 300$ K for a single instant in time (i.e., the replicas are identical here). At high γ, the low correlations at $T_{CD} \simeq 0$ transition into a large "plateau" indicating one distinct phase of the system. Here the partition is almost exclusively composed of dimers and triads of atoms analogous to a gas phase of small non-interacting groups.

In Figs. 3 and 4, our solution for $T_{CD} = 0$ at low $\gamma = 0.001$ resides in another solvable phase. In this region, there is only a weak dependence of the partitions on the heat bath temperature, and the best γ is roughly stable across a large range of heat bath temperatures because the contributions of the repulsive edge weights are greatly reduced. The communities are also stable against the addition of noise (not depicted) indicating that the structures are physical entities as opposed to random constructs. Similar behavior is seen in[43,48] where we observe the identification of planted communities in the presence of noise or real objects in images.

Discussion

We outlined a "first principles" network analysis method to ascertain correlations and structures where traditional tools encounter great difficulty in an important problem. Our key notion is that a general classical physical system may be represented in terms of a (dynamic) network whose links, loops, etc. encode interactions and/or disparate measured multi-particle correlations. We applied the method to detect structures in benchmarks such as disparate lattice systems, with and without defects, Ising spin systems with domain wall structures, (weak) metallic glass formers and binary Lennard Jones systems (see SI). In all of these systems, we are able to identify pertinent structures where the system may be expressed in terms of these building blocks (e.g., the system correlations, energy, and dynamics can be expressed in terms of these reduced degrees of freedom). This identification of pertinent structures in these benchmark systems attests to the physical meaning of this approach. In our model metallic glass of $Al_{88}Y_7Fe_5$, we identify medium range order clusters that overlap neighboring clusters but are weakly coupled with the rest of the system. In this system, strong information theory correlations are found at low temperatures while, as expected, the clusters progressively become less sharply defined as temperature is increased.

We partition the system into strongly correlated cohesive interconnected clusters that are optimally decoupled from other clusters on all determined scales. Although we employed one particular method for network partitioning, other methods may, of course, be applied. To our knowledge, to date, physical systems have not been investigated with graph theoretic concepts. Thus far, analysis of structure has largely relied on various insightful conjectures and on methods that are well suited for simple systems, such as non-interacting gases or periodic crystals, but these may fail in complex (especially multi-component complex) physical systems. The approach that we outline here does not invoke any guesswork. The rudiments of our method can be generally applied to numerous other systems having exact or effective interactions (or measured correlations) between their constituents (e.g., liquids, plasmas, etc.). Although we focused in this work on real space representations, extensions may include representations of the system in Fourier or other spaces. A method such as that presented here may similarly examine the multi-scale structure of other materials such as "phase-change materials," poly-crystalline Silicon, thin films of poly-crystalline CdTe, and similar materials.

More speculative extensions may include electronic and other quantum systems. In the quantum arena, when feasible, a direct product representation in terms of decoupled degrees of freedom (and related matrix product states[53] that efficiently describe cluster states) may be potent. The decomposition into optimally decoupled clusters is indeed what the community detection approach seeks to emulate in the classical systems. Applications to electronic systems such as electronic glasses[54] are also natural. Other applications may offer insights into the long sought diverging length scales (or lack thereof) in strongly correlated electronic systems.

Numerous works, e.g.,[55,56], suggest that a quantum critical point is also present in optimally doped high temperature superconductors. Competing orders and multiple low energy states may lead to a glassy response[57]. As in classical glasses, divergent time scales and various non-uniform structures appear in these complex electronic materials, but the character of the low temperature phases remains a mystery. Generally speaking, a multiresolution approach similar to the one outlined in this work may also be of use for theoretically analyzing non-uniform systems where there are no obvious natural building blocks to consider in performing real space renormalization-group-type calculations and constructing coarse grained effective theories.

Methods

Our potential energy functions for $Al_{88}Y_7Fe_5$ were computed by fitting configuration forces and energies[49] employing *ab initio* results using VASP[50,51]. The calculated structure factors were compared to experimental data[52]. The potentials are of the form

$$V(r) = \left[\left(\frac{a_0}{r}\right)^{a_1} + \frac{a_2}{r^{a_5}}\cos(a_3 r + a_4)\right], \tag{2}$$

with the parameters $\{a_i\}$ depending on the specific types of atom pairs (i.e., Al-Al, Al-Y, …). See the SI for tabulated values[1] of $\{a_i\}$.

We utilized information measures to determine the strengths of replica correlations in our multi-scale analysis[40]. The probability for a randomly selected node to be in community a of partition A is $P(a) = n_a/N$ where n_a is number of nodes in community a and N is the total number of nodes. If there are q communities in partition A, then the Shannon entropy is $H_A = -\sum_{a=1}^{q} \frac{n_a}{N}\log_2\frac{n_a}{N}$. The mutual information $I(A,B)$ between partitions A and B is

$$I(A,B) = \sum_{a=1}^{q_A}\sum_{b=1}^{q_B} \frac{n_{ab}}{N}\log_2\frac{n_{ab}N}{n_a n_b}. \tag{3}$$

q_A and q_B are the number of communities in partitions A and B, respectively, n_{ab} is the number of nodes of community a in partition A that are shared with community b in partition B, and n_b is the number of nodes in community b of partition B. The variation of information VI between two partitions A and B is $VI(A,B) = H_A + H_B - 2I(A,B)$ with a range of $0 \le VI(A,B) \le \log_2 N$. The normalized mutual information NMI is $NMI(A,B) = 2I(A,B)/(H_A + H_B)$ with a range of $0 \le NMI(A,B) \le 1$. A high average NMI or a low average VI indicate strong agreement between the replicas.

After calculating the average replica correlations, we further assigned "overlapping" nodes to the lowest energy partition in order to determine the final clusters. Specifically, we fixed the initial partition configuration (unique node assignments) and iteratively added (or removed) nodes to (from) each cluster k if the change lowered the energy of cluster k. This process repeated until no further overlap changes are detected.

1. Ronhovde, P. *et al.* Detecting hidden spatial and spatio-temporal structures in glasses and complex systems by multiresolution network clustering. *Euro. P. J.* **34**, 105–128 (2011).
2. Anderson, P. W. Through the Glass Lightly. *Science* **267**, 1610 (1995).
3. Miracle, D. B., Miracle, D. B., Sanders, W. S. & Senkov, O. N. The influence of efficient atomic packing on the constitution of metallic glasses. *Phil. Mag.* **83**, 2409–2428 (2003).
4. Miracle, D. B. A structural model for metallic glasses. *Nature Materials* **3**, 697–702 (2004).
5. Schenk, T., Holland-Moritz, D., Simonet, V., Bellissent, R. & Herlach, D. M. Icosahedral short-range order in deeply undercooled metallic melts. *Phys. Rev. Lett.* **89**, 075507 (2002).
6. Kelton, K. F. *et al.* First x-ray scattering studies on electrostatically levitated metallic liquids: Demonstrated inuence of local icosahedral order on the nucleation barrier. *Phys. Rev. Lett.* **90**, 195504 (2003).
7. Lubchenko, V. & Wolynes, P. G. Theory of structural glasses and supercooled liquids. *Annu. Rev. Phys. Chem.* **58**, 235–266 (2007).
8. Angelani, L., Parisi, G., Ruocco, G. & Viliani, G. Potential energy landscape and long-time dynamics in a simple model glass. *Phys. Rev. E* **61**, 1681–1691 (2000).
9. Parisi, G. The physics of the glass transition. *Physica A* **280**, 115–124 (2000).
10. Sastry, S., Debenedetti, P. G. & Stillinger, F. H. Signatures of distinct dynamical regimes in the energy landscape of a glass-forming liquid. *Nature* **393**, 554–557 (1998).
11. Debenedetti, P. G. & Stillinger, F. H. Supercooled liquids and the glass transition. *Nature* **410**, 259–267 (2001).
12. Lubchenko, V. & Wolynes, P. G. Theory of aging in structural glasses. *J. Chem. Phys.* **121**, 2852–2865 (2004).
13. Berthier, L., Biroli, G., Bouchaud, J. P. & Jack, R. L. Overview of difierent characterizations of dynamic heterogeneity. *arXiv:cond-mat/1009.4665.* (2010).

14. Kirkpatrick, T. R., Thirumalai, D. & Wolynes, P. G., Scaling concepts for the dynamics of viscous liquids near an ideal glassy state. *Phys. Rev. A* **40**, 1045–1054 (1989).
15. Tarzia, M. & Moore, M. A. Glass phenomenology from the connection to spin glasses. *Phys. Rev. E* **75**, 031502 (2007).
16. Götze, W. Recent tests of the mode-coupling theory for glassy dynamics. *Journal of Physics: Condensed Matter* **11**, A1 (1999).
17. Mayer, P., Miyazaki, K. & Reichman, D. R. Cooperativity beyond caging: Generalized mode-coupling theory. *Phys. Rev. Lett.* **97**, 095702 (2006).
18. Garrahan, J. P. Glassiness through the emergence of effective dynamical constraints in interacting systems. *J. Phys.: Condensed Matter* **14**, 1571–1579 (2002).
19. Nussinov, Z. Avoided phase transitions and glassy dynamics in geometrically frustrated systems and non-abelian theories. *Phys. Rev. B* **69**, 014208 (2004).
20. Tarjus, G., Kivelson, S. A., Nussinov, Z. & Viot, P. The frustration-based approach of supercooled liquids and the glass transition: a review and critical assessment. *J Phys.: Cond. Matt.* **17**, R1143–R1182 (2005).
21. Falk, M. L. & Langer, J. S. Dynamics of viscoplastic deformation in amorphous solids. *Phys. Rev. E* **57**, 7192–7205 (1998).
22. Kivelson, D., Kivelson, S. A., Zhao, X., Nussinov, Z. & Tarjus, G. A thermodynamic theory of supercooled liquids. *Physica A: Statistical and Theoretical Physics* **219**, 27–38 (1995).
23. Nelson, D. R. *Defects and Geometry in Condensed Matter Physics* (Cambridge University Press, 2002).
24. Sadoc, J. F. & Mosseri, R. *Geometrical Frustration* (Cambridge University Press, 1999).
25. Ritort, F. & Sollich, P. Glassy dynamics of kinetically constrained models. *Adv. Phys.* **52**, 219–342 (2003).
26. Cvetkovic, V., Nussinov, Z. & Zaanen, J. Topological kinematic constraints: dislocations and the glide principle. *Phil. Mag.* **86**, 2995–3020 (2006).
27. Aharonov, E. *et al*. Direct identification of the glass transition: Growing length scale and the onset of plasticity. *Euro. Phys. Lett.* **77**, 56002 (2007).
28. Boolchand, P., Lucovsky, G., Phillips, J. C. & Thorpe, M. F. Self-organization and the physics of glassy networks. *Phil. Mag.* **85**, 3823–3838. (2005).
29. Berthier, L. & Biroli, G. Theoretical perspective on the glass transition and amorphous materials. *Rev. Mod. Phys.* **83**, 587–645 (2011).
30. Chandler, D. & Garrahan, J. P. Dynamics on the way to forming glass: Bubbles in space-time. *Ann. Rev. Phys. Chem.* **61**, 191–217 (2007).
31. Montanari, A. & Semerjian, G. Rigorous inequalities between length and time scales in glassy systems. *J. Stat. Phys.* **125**, 23–54 (2006).
32. Tanaka, H., Kawasakia, T., Shintani, H. & Watanabe, K. Critical-like behaviour of glass-forming liquids. *Nature Mat.* **9**, 324–331 (2010).
33. Berthier, L. *et al.* Direct experimental evidence of a growing length scale accompanying the glass transition. *Science* **310**, 1797–1800 (2005).
34. Bouchaud, J. P. & Biroli, G. On the Adam-Gibbs-Kirkpatrick-Thirumalai-Wolynes scenario for the viscosity increase in glasses. *J. Chem. Phys.* **121**, 7347–7354 (2004).
35. Kurchan, J. & Levine, D. Correlation length for amorphous systems. *arXiv:cond-mat.dis-nn/0904.4850.* (2009).
36. Sheng, H. W., Luo, W. K., Alamgir, F. M., Bai, J. M. & Ma, E. Atomic packing and short-to-medium-range order in metallic glasses. *Nature* **439**, 419–425 (2006).
37. Honeycutt, J. D. & Andersen, H. C. Molecular dynamics study of melting and freezing of small Lennard-Jones clusters. *J. Phys. Chem.* **91**, 4950–4963 (1987).
38. Steinhardt, P. J., Nelson, D. R. & Ronchetti, M. Bond-orientational order in liquids and glasses. *Phys. Rev. B* **28**, 784–805 (1983).
39. Newman, M. E. J. The physics of networks. *Phys. Today* **61**, 33–38 (2008).
40. Ronhovde, P. & Nussinov, Z. Multiresolution community detection for megascale networks by information-based replica correlations. *Phys. Rev. E* **80**, 016109 (2009).
41. Lancichinetti, A. & Fortunato, S. Community detection algorithms: a comparative analysis. *Phys. Rev. E* **80**, 056117 (2009).
42. Ronhovde, P. & Nussinov, Z. Local resolution-limit-free Potts model for community detection. *Phys. Rev. E* **81**, 046114 (2010).
43. Hu, D., Ronhovde, P. & Nussinov, Z. Phase transitions in random Potts systems and the community detection problem: spin-glass type and dynamic perspectives. *Phil. Mag.* **92**, 406-445 (2012).
44. Meilă, M. Comparing clusterings – an information based distance. *J. Multivariate Anal.* **98**, 873–895 (2007).
45. Danon, L., Díaz-Guilera, A., Duch, J. & Arenas, A. Comparing community structure identification. *J. Stat. Mech.: Theory Exp.* **9**, P09008 (2005).
46. Arenas, A., Fernández, A. & Gómez, S. Analysis of the structure of complex networks at different resolution levels. *New J. Phys.* **10**, 053039 (2008).
47. Fortunato, S. Community detection in graphs. *Physics Reports* **486**, 75–174 (2010).
48. Hu, D., Ronhovde, P. & Nussinov, Z. Replica inference approach to unsupervised multiscale image segmentation. *Phys. Rev. E* **85**, 016101 (2012).
49. Mihalkovič, M., Henley, C. L., Widom, M. & Ganesh, P. Empirical oscillating potentials for alloys from ab-initio fits. *arXiv:cond-mat.mtrl-sci/0802.2926.* (2008).
50. Kresse, G. & Hafner, J. Ab initio molecular dynamics for liquid metals. *Phys. Rev. B* **47**, 558–561 (1993).
51. Kresse, G. & Furthmüller, J. Efficient iterative schemes for ab initio total-energy calculations using a plane-wave basis set. *Phys. Rev. B* **54**, 11169–11186 (1996).
52. Sahu, K. *et al.* Phase separation mediated devitrification of Al88Y7Fe5 glasses. *Acta Materialia* **58**, 4199–4206 (2010).
53. Perez-Garcia, D., Verstraete, F., Wolf, M. M. & Cirac, J. I. Matrix product state representations. *Quantum Information and Computation* **7**, 401–430 (2007).
54. Amir, A., Oreg, Y. & Imry, Y. Electron glass dynamics. *Annual Review of Condensed Matter Physics* **2**, 235–262 (2011).
55. Valla, T. *et al.* Evidence for quantum critical behavior in the optimally doped cuprate $Bi_2Sr_2CaCu_2O_{8+\delta}$. *Science* **285**, 2110–2113 (1999).
56. Marel, D. *et al.* Quantum critical behaviour in a high-Tc superconductor. *Nature Lett.* **425**, 271–274 (2003).
57. Park, T. *et al.* Novel dielectric anomaly in the hole-doped $La_2Cu_{1-x}Li_xO_4$ and $La_{2-x}Sr_xNiO_4$ insulators: Signature of an electronic glassy state. *Phys. Rev. Lett.* **94**, 017002 (2005).

Acknowledgments

We are indebted to M. Widom and M. Mihalkovič for help with effective atomic potentials. ZN also wishes to thank G. Tarjus and P. G. Wolynes for critical reading and remarks. This work is partially supported by the National Science Foundation under grants NSF-DMR-1106293 (ZN) and the NSF-KITP-11-030.

Author contributions

PR analyzed the data. SC performed simulations and provided data. DH, MS, and KKS performed research. NM and KFK contributed empirical and simulation data. ZN performed and guided research and provided analytical results. PR, SC, and ZN wrote the main manuscript text. PR and SC generated figures 1 through 5. DH generated figure 6.

Additional information

Supplementary information accompanies this paper at http://www.nature.com/scientificreports

Competing financial interests: The authors declare no competing financial interests.

How to cite this article: Ronhovde, P. *et al.* Detection of hidden structures for arbitrary scales in complex physical systems. *Sci. Rep.* **2**, 329; DOI:10.1038/srep00329 (2012).